Microbubble Oscillation due to Harmonic, Pulsed and Frequency Modulated Excitation with Ultrasound

Tobias Gehrke, Heinrich M. Overhoff

Medical Engineering Laboratory, University of Applied Sciences Gelsenkirchen
tobias.gehrke@fh-gelsenkirchen.de

Abstract. Improved visualization of blood vessels by ultrasound contrast agents requires insonation that is adapted to the dynamics of the contrast agent bubbles. To evaluate the interrelation between parameters of the exciting pressure field and the contrast agent, the dynamics of air filled microbubbles immersed in water are examined by numerical evaluation of the Rayleigh-Plesset equation. Unsymmetrical oscillation is obtained for resonant harmonic excitation, frequency doubling occurs for subresonant excitation and nearly sinusoidal oscillation is exhibited for superresonant excitation. Continuous harmonic and pulsed pressure waves are shown to be unsuitable to excite a mixture of differently sized bubbles due to their non-uniform resonance behaviour. As an alternative, excitation with a linear frequency modulated wave is examined and shown to be a feasible option for adapted contrast agent insonation.

1 Introduction

Segmentation of vessels within an ultrasound image is a prerequisite for automatic image analysis or three dimensional visualization in vascular applications. Small vessels can frequently not clearly been identified in an ultrasound image since they appear buried between stronger echogenic surrounding tissue. Automatic segmentation of those vessels can be simplified by the use of ultrasound contrast agents which significantly enhance the echo amplitudes. Further improvement can be achieved by specifically adapted imaging algorithms such as harmonic imaging or pulse inversion that make use of the contrast agent's nonlinear behaviour [1].

Ultrasound contrast agents are realized as gas-filled microbubbles. The radii of these bubbles oscillate when exposed to sonic waves emitted from an ultrasound transducer [1, 2, 3]. While the bubble's oscillation is nearly linear for small exciting pressures, higher pressures cause asymmetric oscillation and thereby nonlinear bubble dynamics. These asymmetric oscillations are due to a reduced compressibility of the filling gas with decreasing bubble bubble radius.

In order to create oscillation amplitudes large enough to be detected at the body surface by the transducer in receive mode, additionally to a sufficiently high amplitude, the frequency of the exciting wave must be adjusted to the

resonance properties of the bubbles [4]. Furthermore, careful adaption of the signal processing i.e. imaging algorithm to the specific nonlinear bubble oscillation can increase the visibility of small vessels. Therefore realistic simulation of the bubble dynamics is a crucial task in the development of contrast agent imaging modalities.

In this paper, the oscillations of air-filled microbubbles in water due to harmonic resonant, subresonant and superresonant forcing as well as due to pulsed and frequency modulated excitation are examined. Real contrast agents consist of a mixture of differently sized bubbles, which hence show non-uniform resonance behaviour. The consequences for parameters of the exciting wave are examined and a proper setting is derived.

2 Materials and Methods

The dynamic behaviour of a single spherically symmetrical gas-bubble immersed in an incompressible fluid can be modelled by a nonlinear differential equation of second order, called Rayleigh-Plesset equation [1, 3]. Properties of the numerical solver and results for defined physical wave propagation and bubble parameters are investigated.

2.1 Rayleigh-Plesset Dynamics

The Rayleigh-Plesset equation

$$\bar{\rho}\left(R(t)\ddot{R}(t)+\tfrac{3}{2}\dot{R}(t)^2\right)= \left(p_0+\frac{2\sigma}{R_0}-p_\mathrm{v}\right)\left(\frac{R_0}{R(t)}\right)^{3\gamma}-\frac{2\sigma+4\eta\dot{R}(t)}{R(t)}+p_\mathrm{v}-\big(p_0+\Delta p(t)\big) \quad (1)$$

relates outer pressure changes $\Delta p(t)$ to a time varying bubble radius $R(t)$. Under equilibrium conditions $\Delta p(t)=0$, the pressure inside the surrounding liquid is p_0. The static bubble radius under equilibrium conditions is $R(t)=R_0$. The surrounding liquid is characterized by its density ρ, dynamic viscosity η, and vapour pressure p_v. The quantity σ is the surface tension of the liquid-gas interface, and γ denotes the polytropic exponent of the gas inside the bubble.

2.2 Numerical Solver

The Rayleigh-Plesset equation has been implemented in Matlab (The Mathworks Inc., Natick, MA, USA) and numerically solved in the time domain using a variable order BDF (backward differentiation formula) method. The algorithm uses a variable step size Δt that depends on the local rate of change of the solution. This enables detection of quasi-discontinuities as they occur when the bubble radius $R(t)$ approaches zero. Cubic spline interpolation of the solution advances processing steps that require regularly sampled data such as the discrete Fourier transform.

Table 1. Characteristic values of gas (air) and surrounding liquid (water) that have been used for the simulation

Liquid pressure	p_0	100 kPa
Liquid density	ρ	998 kg/m^3
Dynamic liquid viscosity	η	1 mPa
Vapour pressure	p_v	5945 Pa
Surface tension	σ	72.5 mN/m
Polytropic exponent	γ	1

2.3 Simulation Settings

The equation parameters have been set to model an air filled bubble immersed in water at ambient temperature and pressure. Adiabatic gas behaviour $\gamma = 1$ has been assumed. An overview of the simulation settings is given in Tab. 1.

3 Results

The modelled bubble of equilibrium radius $R_0 = 2.26\,\mu m$ exhibits a nonlinear resonance frequency $f_{\mathrm{exc}} = 1260\,\mathrm{kHz}$. In Fig. 2(a) resonant bubble dynamics is visualized in the phase plane for harmonic excitation

$$\Delta p_{\mathrm{har}}(t) = \Delta p_0 \sin(2\pi f_{\mathrm{exc}} t) \tag{2}$$

with $\Delta p_0 = 36\,\mathrm{kPa}$. The steady state phase diagram for excitation of the first and second subharmonic and the first harmonic is shown in Fig. 2(b). The figures reveal that frequency doubling occurs for frequencies below resonance, while excitation with the first harmonic frequency causes nearly sinusoidal oscillation. Simple albeit unsymmetrical oscillation occurs for excitation at resonance. Approaching the minimal bubble radius coincides with a large oscillation velocity. Unsymmetrical oscillation and frequency doubling can also be clearly obtained in the time domain as is shown in Fig. 2, where the varying bubble radius is depicted as a function of time for excitation with the resonance frequency and half the resonance frequency.

Harmonic pressure waves excite only bubbles of distinct size, as can be seen in Fig. 3 where the relative amplitude of oscillation $\Delta R/R_0$ with $\Delta R = \max\big(R(t)\big) - \min\big(R(t)\big)$ is charted as a function of the equilibrium bubble radius R_0 for continuous harmonic excitation with frequency $f_{\mathrm{exc}} = 1260\,\mathrm{kHz}$ (black line). The oscillation amplitude rises very sharply towards its maximum at the resonance radius $R_0 = 2.26\,\mu m$, while the falling edge of the curve is less steep such that considerable oscillation occurs for a small band of radii above the resonance radius. Radii around $R_0 = 4.65\,\mu m$ show harmonic oscillation due to the excitation frequency $f_{\mathrm{exc}} = 1260\,\mathrm{kHz}$. Also subharmonic excitation of bubbles with radii around$R_0 = 1.4\,\mu m$ can be noticed.

Pressure pulses that normally excite bubbles in pulse echo ultrasound imaging have a broader frequency content and are thus capable to excite bubbles of a

Fig. 1. Phase diagrams of bubble oscillations. (a) Oscillation at resonance $f_{\mathrm{exc}} = 1260\,\mathrm{kHz}$. (b) Oscillation for excitation with $f_{\mathrm{exc}} = 420\,\mathrm{kHz}$ (black line), $f_{\mathrm{exc}} = 630\,\mathrm{kHz}$ (dark grey line), $f_{\mathrm{exc}} = 2520\,\mathrm{kHz}$ (light grey line)

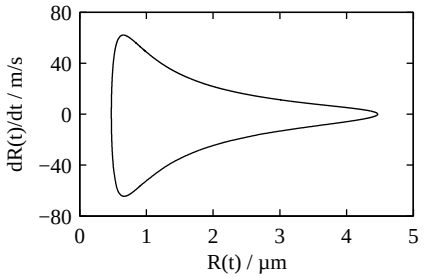

(a)

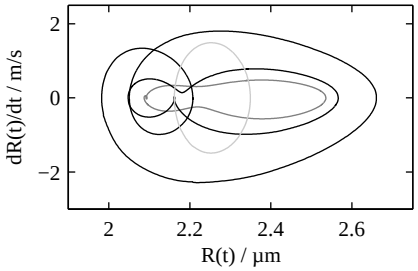

(b)

Fig. 2. Bubble radii $R(t)$ as functions of time t for resonant excitation $f_{\mathrm{exc}} = 1260\,\mathrm{kHz}$ (black line) and subharmonic excitation $f_{\mathrm{exc}} = 630\,\mathrm{kHz}$ (grey line)

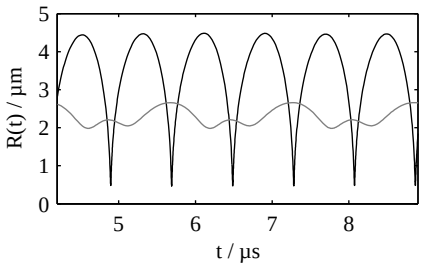

Fig. 3. Relative amplitudes of oscillations $\Delta R/R_0$ as functions of the equilibrium bubble radius R_0 due to continuous harmonic excitation (black line) and pulsed excitation (dark grey line) with frequency $f_{\mathrm{exc}} = 1260\,\mathrm{kHz}$, and due to excitation with a chirp signal whose frequency rises from $f_{\mathrm{exc1}} = 300\,\mathrm{kHz}$ to $f_{\mathrm{exc2}} = 3000\,\mathrm{kHz}$ (light grey line)

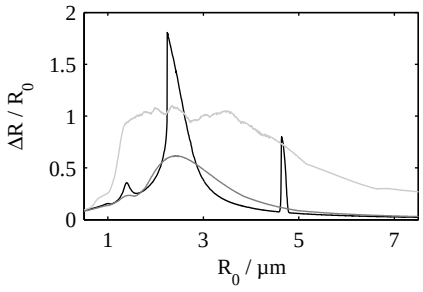

greater radius range than harmonic excitation does. In Fig. 3 the dark grey line shows relative oscillation amplitudes due to excitation with a sinusoidal pulse of $f_{\mathrm{exc}} = 1260\,\mathrm{kHz}$ and three periods length tapered by a Hann window.

The light grey curve in Fig. 3 shows the relative oscillation amplitudes due to excitation with a chirp signal

$$\Delta p_{\mathrm{crp}}(t) = \Delta p_0 \sin\left(2\pi\left(f_{\mathrm{exc1}} + \frac{f_{\mathrm{exc2}} - f_{\mathrm{exc1}}}{2T}t\right)t\right) \tag{3}$$

whose frequency rises linearly from $f_{\mathrm{exc1}} = 300\,\mathrm{kHz}$ to $f_{\mathrm{exc2}} = 3000\,\mathrm{kHz}$. The signal amplitude and duration are $\Delta p_0 = 36\,\mathrm{kPa}$ and $T = 12.1\,\mu s$ respectively.

The signal edges have been tapered to resemble smooth start and ending of signals from real, bandlimited ultrasound systems. Comparison of the three curves in Fig. 3 reveals that - in contrast to harmonic or pulsed excitation - the chirp signal is capable to excite an ensemble of differently sized contrast agent bubbles if its spectrum is adapted to the radius distribution.

4 Discussion

A single microbubble shows distinct resonant behaviour, with moderate excitation pressures causing large oscillation amplitudes. Simulations show that amplitudes at resonance are of the same order as those for subresonant excitation.

In the more realistic case of an ensemble of bubbles with different sizes, harmonic or pulsed pressure waves excite only a small subset of these bubbles. Broadband signals with sufficient energy such as chirp signals proved to excite more bubbles. The application of long duration broadband signals requires pulse compression during the image formation process. For linear pulse echo imaging this task can successfully be accomplished by matched filters [5]. Matched filtering is however not directly adaptable for contrast agent enhanced imaging, since the nonlinear response of the bubbles can not be handled.

The simulations give a general impression about the dynamics of ultrasound contrast agent bubbles. A more realistic model must include the influence of the bubble shells [6, 7], the interrelation between the members of a bubble ensemble, and spherically asymmetric bubbles.

References

1. Szabo TL. Diagnostic Ultrasound Imaging. Elsevier, Amsterdam; 2004.
2. Jong ND, Cornet R, Lancée CT. Higher harmonics of vibrating gas-filled microspheres. Ultrasonics. 1994;32(6):447–53.
3. Hilgenfeldt S, Lohse D, Zomack M. Response of bubbles to diagnostic ultrasound: A unifying approach. Eur Phys J B. 1998;4(2):247–55.
4. Mukdadi OM, Kim HB, Hertzberg J, et al. Numerical modeling of microbubble backscatter to optimize ultrasound particle image velocimetry imaging: Initial studies. Ultrasonics. 2004;42:1111–21.
5. Misaridis T, Jensen JA. Use of modulated excitation signals in medical ultrasound. Part I: basic concepts and expected benefits. IEEE Trans Ultrason Ferroelectr Freq Control. 2005;52(2):177–91.
6. Church CC. The effects of an elastic solid surface layer on the radial pulsations of gas bubbles. J Acoust Soc Am. 1995;97(3):1510–21.
7. Hoff L, Sontum PC, Hovem JM. Oscillations of polymeric microbubbles: effect of the encapsulating shell. J Acoust Soc Am. 2000;107(4):2272–80.